



A Supramolecular Interaction of a Ruthenium Complex With Calf-Thymus DNA: A Ligand Binding Approach by NMR Spectroscopy

Flávio Vinícius Crizóstomo Kock¹, Analu Rocha Costa², Katia Mara de Oliveira², Alzir Azevedo Batista², Antônio Gilberto Ferreira¹ and Tiago Venâncio^{1*}

¹ Laboratory of Nuclear Magnetic Resonance, Department of Chemistry, Federal University of São Carlos, São Carlos, Brazil, ² Laboratory of Structure and Reactivity of Inorganic Compounds, Department of Chemistry, Federal University of São Carlos, São Carlos, Brazil

OPEN ACCESS

Edited by:

Enrica Calleri,
University of Pavia, Italy

Reviewed by:

Francesco Crea,
University of Messina, Italy
Qifeng Li,
Tianjin University, China

*Correspondence:

Tiago Venâncio
venancio@ufscar.br

Specialty section:

This article was submitted to
Analytical Chemistry,
a section of the journal
Frontiers in Chemistry

Received: 23 July 2019

Accepted: 23 October 2019

Published: 08 November 2019

Citation:

Kock FVC, Costa AR, de Oliveira KM, Batista AA, Ferreira AG and Venâncio T (2019) A Supramolecular Interaction of a Ruthenium Complex With Calf-Thymus DNA: A Ligand Binding Approach by NMR Spectroscopy. *Front. Chem.* 7:762. doi: 10.3389/fchem.2019.00762

Lawsone itself exhibits interesting biological activities, and its complexation with a metal center can improve the potency. In this context a cytotoxic Ru-complex, [Ru(law)(dppb)(bipy)] (law = lawsone, dppb = 1,4-bis(diphenylphosphino)butane and bipy = 2,2'-bipyridine), named as CBLAU, was prepared as reported. In this work, NMR binding-target studies were performed to bring to light the most accessible interaction sites of this Ru-complex toward Calf-Thymus DNA (CT-DNA, used as a model), in a similar approach used for other metallic complexes with anti-cancer activity, such as cisplatin and carboplatin. Advanced and robust NMR binding-target studies, among them Saturation Transfer Difference (STD)-NMR and longitudinal relaxometry (T_1), were explored. The ^1H and ^{31}P -NMR data indicate that the structure of Ru-complex remains preserved in the presence of CT-DNA, and some linewidth broadening is also observed for all the signals, pointing out some interaction. Looking at the binding efficiency, the T_1 values are highly influenced by the formation of the CBLAU-DNA adduct, decreasing from 11.4 s (without DNA) to 1.4 s (with DNA), where the difference is bigger for the lawsone protons. Besides, the STD-NMR titration experiments revealed a stronger interaction ($K_D = 5.9\text{ mM}$) for CBLAU-DNA in comparison to non-complexed lawsone-DNA ($K_D = 34.0\text{ mM}$). The epitope map, obtained by STD-NMR, shows that aromatic protons from the complexed lawsone exhibits higher saturation transfer, in comparison to other Ru-ligands (DPPB and bipy), suggesting the supramolecular contact with CT-DNA takes place by the lawsone face of the Ru-complex, possibly by a spatial π - π stacking involving π -bonds on nucleic acids segments of the DNA chain and the naphthoquinone group.

Keywords: binding interactions, lawsone, ruthenium complex, anti-cancer, CT-DNA, NMR

INTRODUCTION

Cancer is among the major public health problems worldwide and is responsible for millions of deaths, only in the United States (Siegel et al., 2019). Many biological macromolecular targets are involved in the complex mechanism of the cancer development, and nucleic acids, such as DNA, are one of these targets. The action of traditional chemotherapeutics based on metallic complexes

(metallo-drugs), for example cisplatin and carboplatin, involves their interaction with the DNA. Hence, the search for new metallic complexes with anti-tumor activity is one of the most important research fields in bioinorganic chemistry. Regarding this action mechanism, studies aiming to deep the knowledge about the intermolecular interaction between new potential drugs and biological targets are relevant, because it leads the design of new potent and selective anti-cancer candidates.

A strategy used to design new chemotherapeutics candidates and improve its anti-tumoral activity, consists on the complexation of some metallic centers, among them, silver (I) (Ali et al., 2013; Engelbrecht et al., 2018; Hussaini et al., 2019), gold (I)/(III) (Yeo et al., 2018; Dabiri et al., 2019; Hussaini et al., 2019), copper (II) (Khan et al., 2017; Zhang et al., 2018; Chen et al., 2019), and platinum (II) (Hua et al., 2019; Hussaini et al., 2019; Makovec, 2019) with a wide-range of ligands and also with natural molecules that already demonstrate some anti-cancer features, such as quinoline, flavones, and naphthoquinones (Kosmider and Osiecka, 2004; Lu et al., 2016; Oliveira et al., 2017a; Wang et al., 2018; Grandis et al., 2019). In this scenario, ruthenium takes special interests due to the possibility to reach several different metallic-arrangements, supplying distinct reactivities and applications (Oliveira et al., 2017b; Hussaini et al., 2019; Roy et al., 2019).

In this work, the ligand (2-hydroxy-1,4-naphthoquinone), a naphthoquinone with anti-viral, anti-fungal, anti-parasitic, anti-microbial, and anti-cancer biological features well-described in literature (Oliveira et al., 2017a) and the Ru/lawsone complex, [Ru(law)(dppb)(bipy)] (law = lawsone, dppb = 1,4-bis(diphenylphosphino)butane and bipy = 2,2'-bipyridine), named as CBLAU were fully investigated by NMR spectroscopy. The action of this potential metallo-drug against tumor cell lines, among them, DU-145 (prostate cancer cells), MCF-7 (breast cancer cells), A549 (lung cancer cells) founds reported in the literature as well as its potential to induce the tumor cells apoptosis (Oliveira et al., 2017a). Considering that for all these cases, DNA is a possible and relevant biological target, similarly that occurs for cisplatin and/or carboplatin that acts binding covalently with pairs of nitrogenous DNA bases (Oliveira et al., 2017a), the intermolecular interaction of this new candidate (CBLAU) toward this biological target, is investigated in this research. In this work the intermolecular binding interactions will be investigated by NMR approaches, aiming to probe the intermolecular contact in the atomic level. These efforts can be reached using NMR techniques able to provide a reliable answer at molecular level (Viegas et al., 2011; Tanoli et al., 2015, 2018; Monaco et al., 2018).

Among several other techniques used for probing binding-targets interaction, among them circular dichroism, viscosimetry, and fluorescence (Oliveira et al., 2017a,b, 2019; Villareal et al., 2017; Gagini et al., 2018; Grandis et al., 2019), NMR-based methods is a unique spectroscopy able to supply in atomic level reliable answers for binding affinities studies in aqueous media (Tanoli et al., 2015, 2018). In addition, this experimental approach requires a very low concentration of protein without isotopic labeling, with any prior knowledge of its structure and/or function and does not have restriction on the protein size (Mayer and Meyer, 1999, 2001; Angulo et al., 2010; Angulo

and Nieto, 2011; Viegas et al., 2011; Monaco et al., 2018). Based on the aforementioned features, these NMR experiments are the most routinely used techniques for drug/biological target recognition processes, through the knowledge about the spatial interaction, binding epitope mapping (GEM), and determination of dissociation constants (K_D), supplying an unequivocal grasp about the intermolecular interactions, where most of the others analytical methods are unable to provide satisfactory answers (Mayer and Meyer, 1999, 2001; Angulo et al., 2010; Angulo and Nieto, 2011; Viegas et al., 2011; Monaco et al., 2018; Nepravishta et al., 2019).

Therefore, herein, we use NMR binding-target interaction approaches, among them ^1H - and ^{31}P -NMR, relaxometric experiments, Saturation Transfer Difference (STD)-NMR for scrutiny at atomic level the intermolecular interaction between the potential anti-cancer candidate (CBLAU) toward DNA. To the best of our knowledge few papers devote special attention on a detailed application of NMR spectroscopy to characterize the interaction of metallic complexes with macromolecular targets. As a result, we expect to introduce detailed NMR studies in order to open a new possibility of frontiers researches in bioinorganic chemistry, aiming to rationalize the designing of new metallo-drugs based chemotherapeutics, with improved potency and selectivity against cancer, which still remains a challenge.

EXPERIMENTAL

Sample Preparation

Calf-thymus DNA (CT-DNA) was purchased from Sigma-Aldrich Ltd (Brazil) and used without previous purification. A 1.078 mM solution of CT-DNA was prepared by dissolving an adequate weight of this macromolecule in a deuterated phosphate buffer. The pH 7.2 phosphate D_2O buffer was prepared by dissolving disodium hydrogen phosphate ($\text{Na}_2\text{HPO}_4 \cdot 12\text{H}_2\text{O}$, 0.1180 g) and sodium dihydrogen phosphate ($\text{NaH}_2\text{PO}_4 \cdot 2\text{H}_2\text{O}$, 0.0217 g) in 10.00 mL D_2O (99.9%, Cambridge Isotopes Laboratories, Inc. with pH 7.2) to make a 0.046 M solution. The (CBLAU)(BF_4^-) complex was dissolved in a 5:95% v/v of DMSO (99.8% Cambridge Isotopes Laboratories, Inc.) and deuterated buffer respectively. BF_4^- was used as a counter ion together with 5% of DMSO- d_6 to increase the solubility of the Ru-complex in aqueous solution. All ^1H NMR and STD-NMR spectra were recorded using a 1:100 (DNA:CBLAU) molar ratio, in a final volume of 500 μL transferred to a 5 mm NMR tube (Norrel, Inc. USA). For the epitope mapping experiment, the final concentration of CBLAU was 5 mM and the concentration for the CT-DNA was 50 μM . On the other hand, for the concentration-dependent STD-NMR experiment, the CBLAU and lawsone concentrations were ranged from 5 to 1 mM. In these experiments, the CT-DNA concentration was fixed in 50 μM . For these studies, 7 independent STD-NMR experiments were acquired for each concentration.

NMR Spectroscopy

All ^1H -NMR based experiments were recorded on a Bruker Avance III 14.1 T spectrometer equipped with a TCI cryoprobe and the ^{31}P -NMR experiments were performed on a Bruker

Avance III 9.4 T spectrometer. The proton resonance frequencies for both magnetic fields are 600 and 400 MHz, respectively. Data acquisition and processing were performed with the Bruker software Topspin 3.5 pl. 7 version installed in the spectrometer. All the experiments were done at 298 K.

One-Dimensional NMR (^1H and ^{31}P Experiments)

The ^1H -spectra were acquired using a standard Bruker presaturation pulse sequence (zgesgp) pulses length of 9.57 us and 19.14 us for the 90° and 180° , respectively, with a gradient length pulse of 2,000 us. Besides, other experimental conditions were acquisition time of 4.63 s (32 K points), recycle delay of 4 s, spectral window of 20.02 ppm, and accumulation of 128 transients. For the acquisition of ^{31}P -spectra a standard BRUKER pulse sequence (zgpg30) was used with a pulse length of 25.0 us and 50 us for the 90° and 180° , respectively. In addition, a spectral width of 289.40 ppm, recycle delay of 0.1 s (32 K points) were used and a total of 131,072 transients were co-added.

Relaxometric Experiments

The relaxometric experiments were acquired using the standard Bruker pulse sequence inversion-recovery (tir), spectral window of 15.01 ppm, acquisition time of 1.8 s (32 K points), pulses lengths of 9.35 us and 18.70 us for the 90° and 180° , 16 transients and exponentially ranging the time between the pulses (τ) from 0.001 to 30 s. For the longitudinal relaxation time (T_1) constant determination, was used the monoexponential fitting for the experimental obtained data, using for this purpose the software Topspin 3.5 pl.7.

STD-NMR

These experiments were recorded by using a Bruker standard pulse sequence with water suppression (stdiffesgp.3), with a pseudo-2D setup through an intervalled acquisition of an *on*- and *off*-resonance experiment. The water suppression was done under excitation sculpting scheme, properly optimized. Selective irradiation (during saturation time) of CT-DNA was achieved using a train of soft Gaussian-shaped pulses, with attenuation level of 45–55 dB, 50 ms of length and separated by a 2 ms interval. The frequency chosen for an adequate selective irradiation of CT-DNA was 2289.266 Hz (3.8 ppm) for *on*-resonance and 30,000 Hz (50 ppm) for *off*-resonance. The STD build up curve was acquired by ranging the saturation time between 0.5 and 10 s, and recording 14 independent experiments. Finally, the STD amplification factor (A_{STD}) was calculated by accounting the signal intensity of the STD difference spectrum relative to the reference (*off*-resonance) according to Equation (1; Mayer and Meyer, 1999).

$$A_{STD} = \frac{I_0 - I_{STD}}{I_0} \times \frac{[L]}{[P]} \quad (1)$$

For the determination of the relative percentage of A_{STD} , the proton signal with biggest integral area received the value of 100% and the other signals were normalized with respect to this signal. For the dissociation constant (K_D) estimation, seven STD-NMR

concentration-based experiments were performed. The results were plotted using the Equation 2, and the reciprocal of this equation (Lineweaver-Burk plot) was employed for estimation of K_D .

$$A_{STD} = \frac{\alpha_{STD}[L]}{K_D + [L]} \quad (2)$$

In this equation, A_{STD} corresponds to STD signal intensity, α_{STD} is the maximum STD intensity assuming infinite concentration, and $[L]$ is the ligand concentration. After getting the A_{STD} and α_{STD} values, the curves A_{STD} vs. concentration were built up, linearized and fitted using a linear fit employing the MS Excel (2007) and plotted using the software Origin, version 8.0.

RESULTS AND DISCUSSIONS

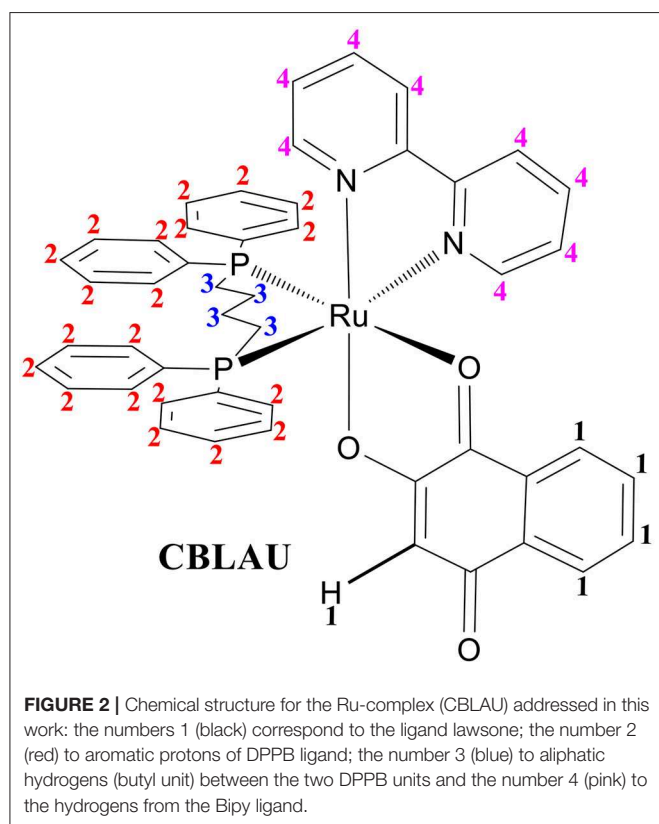
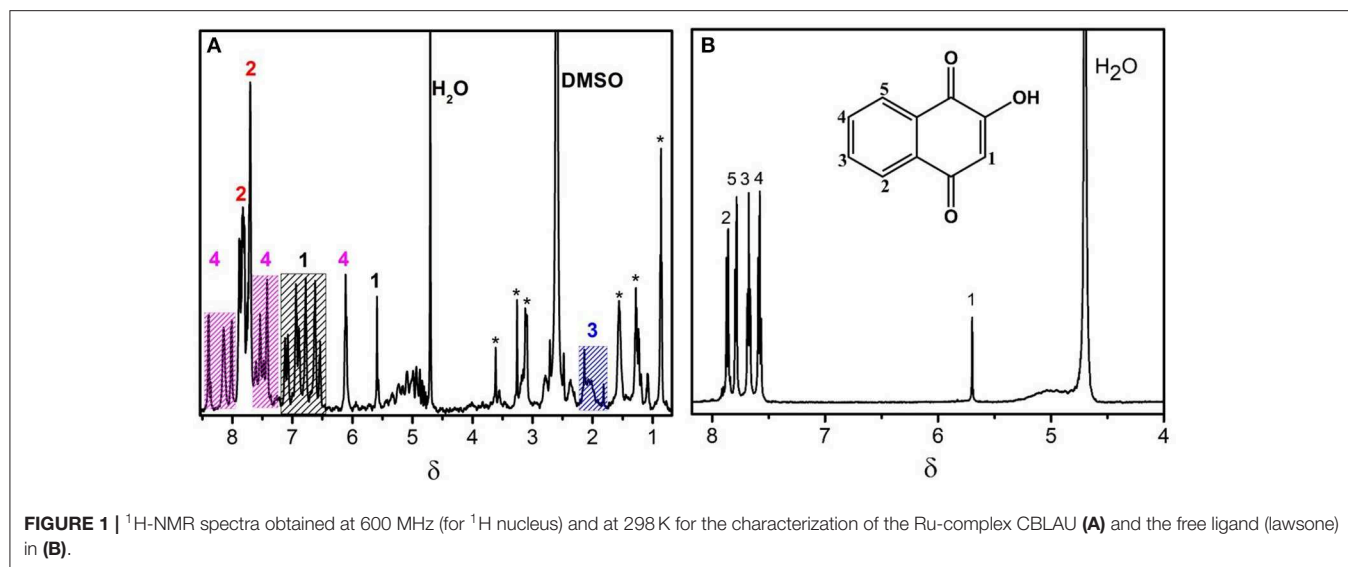
Signal Assignment

The ^1H NMR signal assignment for CBLAU and lawsone are shown in **Figures 1A,B**, respectively. Due to the aromatic character of the ligands, the NMR region above 6.5 ppm at **Figure 1A** exhibits a series of superimposed signals. Despite this spectral feature, the signal discrimination can be done regarding each individual ligand. The set of signals numbered as 1 (black), from 6.8 to 7.4 ppm and at 5.7 ppm, correspond to aromatic hydrogens from lawsone ligand. Moreover, the intense signals assigned by the number 2 (red), from 7.6 to 7.9 ppm are attributed to hydrogens present on DPPB ligand. The signals numbered by 3 (blue), close to 2.0 ppm correspond to aliphatic hydrogens (butyl unit) present on DPPB ligand. To conclude, the set of signals numbered as 4 (pink), above 8.0 ppm and from 7.5 to 7.8 ppm, correspond to hydrogens from Bipy ligand. The presence of some impurities can be observed by the signals assigned with asterisks. These impurities remain even after the laborious process of CBLAU purification. Despite the presence of these residues, they do not interfere in the interaction between CBLAU and CT-DNA, as it will be shown in the following discussions. The **Figure 1B** shows the ^1H -NMR spectrum for the lawsone ligand. On this spectrum, it is clearly possible to observe 5 signals. The hydrogens 2–5 correspond to the aromatic from 7.5 to 7.8 ppm, as indicated. The signal at 5.7 ppm corresponds to vinylic proton, assigned by the number 1.

On **Figure 2** the ^1H NMR signal assignment can be better visualized on the chemical structure for CBLAU, highlighting the chemical groups responsible for each signal observed on the NMR spectra previously presented in the **Figure 1A**. The set of these results (**Figures 1, 2**) will be helpful on the subsequent binding target elucidation studies, providing an atomic comprehension about the contribution of each ligand group present on CBLAU and lawsone responsible by the efficient intermolecular interaction toward the CT-DNA strand.

Interaction With Calf Thymus DNA

In the first approach (**Figure 3**), the ^1H -NMR spectra were obtained for the Ru-complex CBLAU in the presence of CT-DNA (red) and without CT-DNA (black) aiming to reach a preliminary picture about the interactions, based on some chemical shift variation and/or linewidth broadening. Interestingly, it is not

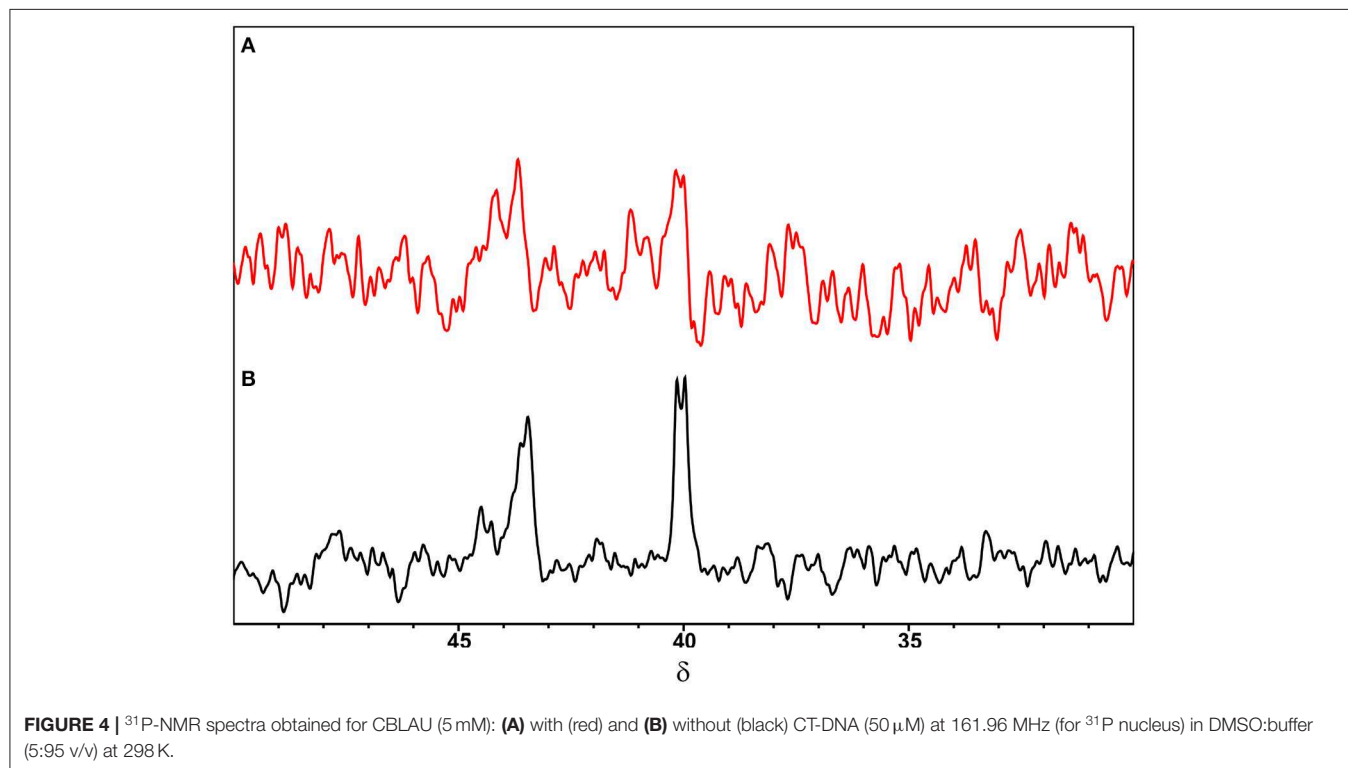
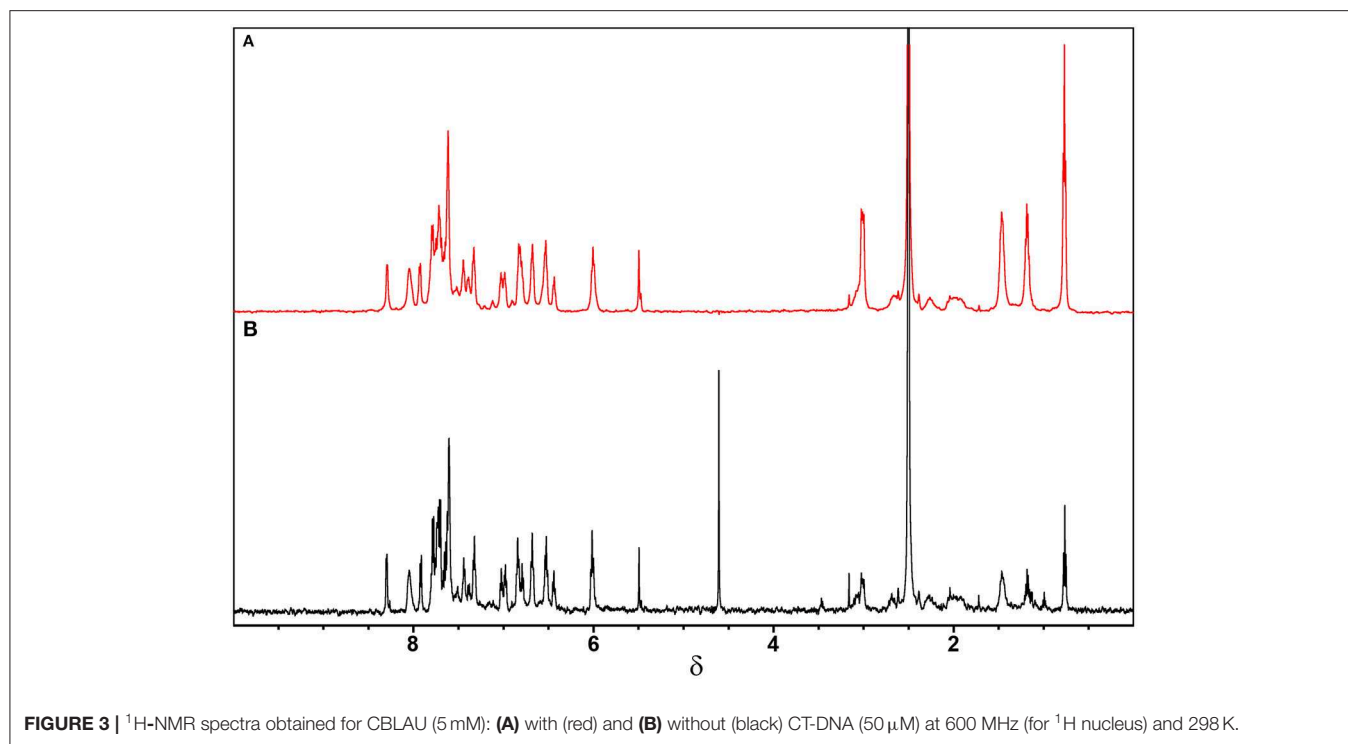


observed any significant change in the NMR spectrum profile due to the presence of DNA. Some linewidth broadening is observed on the spectrum without CT-DNA (black) can be attributed to the complex size, its low solubility and the presence of some quadrupolar component present on some active NMR Ru-isotopes (Levitt, 2008; Keller, 2011). In the presence of CT-DNA, any change can be observed.

Regarding these ¹H-NMR results, the intermolecular interaction between CBLAU toward CT-DNA was investigated by ³¹P-NMR, aiming to scrutiny the influence of presence of CT-DNA on the DPPB ligand, and the preservation of the Ru-complex. For this purpose, two ³¹P-NMR spectra for CBLAU were collected, with and without CT-DNA. The resulting spectra are shown on the **Figure 4**. In the black line it can be observed the ³¹P-NMR signal obtained for the CBLAU at 298 K in DMSO:buffer (5:95 v/v), without CT-DNA. The spectrum in red represents the ³¹P-NMR signal obtained for CBLAU in the presence of CT-DNA. By comparing the spectra, it is clearly observed that the presence of the macromolecule is responsible for the increasing of the ³¹P linewidth. Besides, the signal intensity is reduced, leading to confirm that the interaction between CBLAU and CT-DNA is highly important and demonstrate that for this case, ³¹P-NMR is more sensitive to investigate this binding interaction in comparison to ¹H-NMR.

Therefore, from the analysis of ¹H-NMR spectra it is possible to suggest that the interaction of CBLAU with CT-DNA is weak and possibly takes place through a spatial van-der-Waals intermolecular force. In fact, this type analysis is very preliminary and not conclusive, since the chemical shift variation, as well as the linewidth broadening, can be related to several other effects, such as pH and temperature variation. To circumvent this limitation other robust NMR methods can be better explored, such as NMR-relaxometry and STD-NMR for discriminate at atomic level the binding target intermolecular interactions. These NMR approaches will be explored in the later discussions.

The relaxometric, and particularly the longitudinal relaxation time, is highly useful as a preliminary estimative about the binding-target efficiency, since the longitudinal relaxation times vary according to changes in the molecular mobility. For this purpose, ¹H T₁ relaxation times were determined for the Ru-complex CBLAU with and without CT-DNA. The experimental data showed that the average longitudinal relaxation (T₁) obtained for CBLAU (11.41 s) is highly influenced, due to the



final CBLAU/CT-DNA adduct formation (1.40 s) in solution. These variations can be attributed to the reduction on the molecular mobility associated to CBLAU under the presence of CT-DNA, which is an extremely large macromolecule (8.41×10^6

$\text{g}\cdot\text{mol}^{-1}$) that increases the viscosity of the solution (Porsch et al., 2009). Therefore, these results point out that CBLAU interacts with CT-DNA. The detailed results are listed on **Table 1**, for all the groups complexed with metallic center. The complexed

TABLE 1 | ^1H T_1 relaxation times determined for the Ru-complex CBLAU in solution (5 mM) and in the presence of CT-DNA (50 μM). Results collected at 298 K (600 MHz).

Group	T_1 (s) with CT-DNA	T_1 (s) without CT-DNA	ΔT_1 (s)
Lawsone	1.4	11.5	10.1
Bipy	1.1	11.4	10.3
DPPB	1.4	11.1	9.7
Butane branch	1.8	11.6	9.8

lawsone and bipyridine are mostly affected by the presence of CT-DNA and these findings indicate that these groups exhibit a shorter contact with CT-DNA surface. The formation of the supramolecular adducts, CBLAU/CT-DNA obeys a binding equilibrium, where the lawsone and bipy face of CBLAU seems to be more involved in the intermolecular contact.

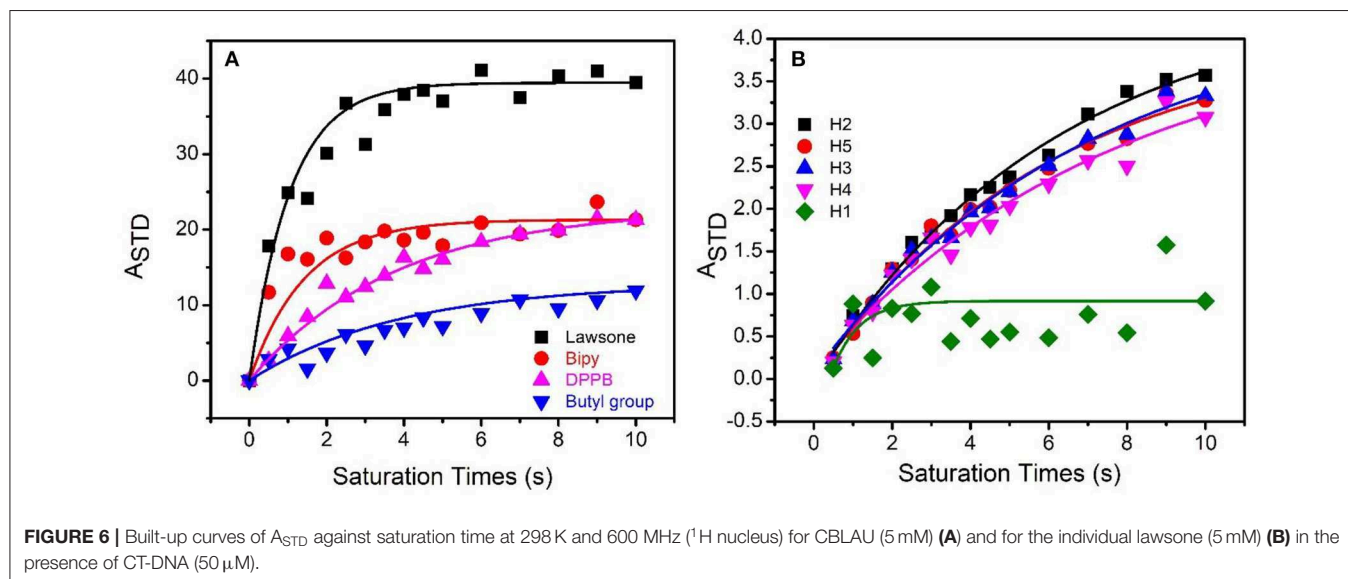
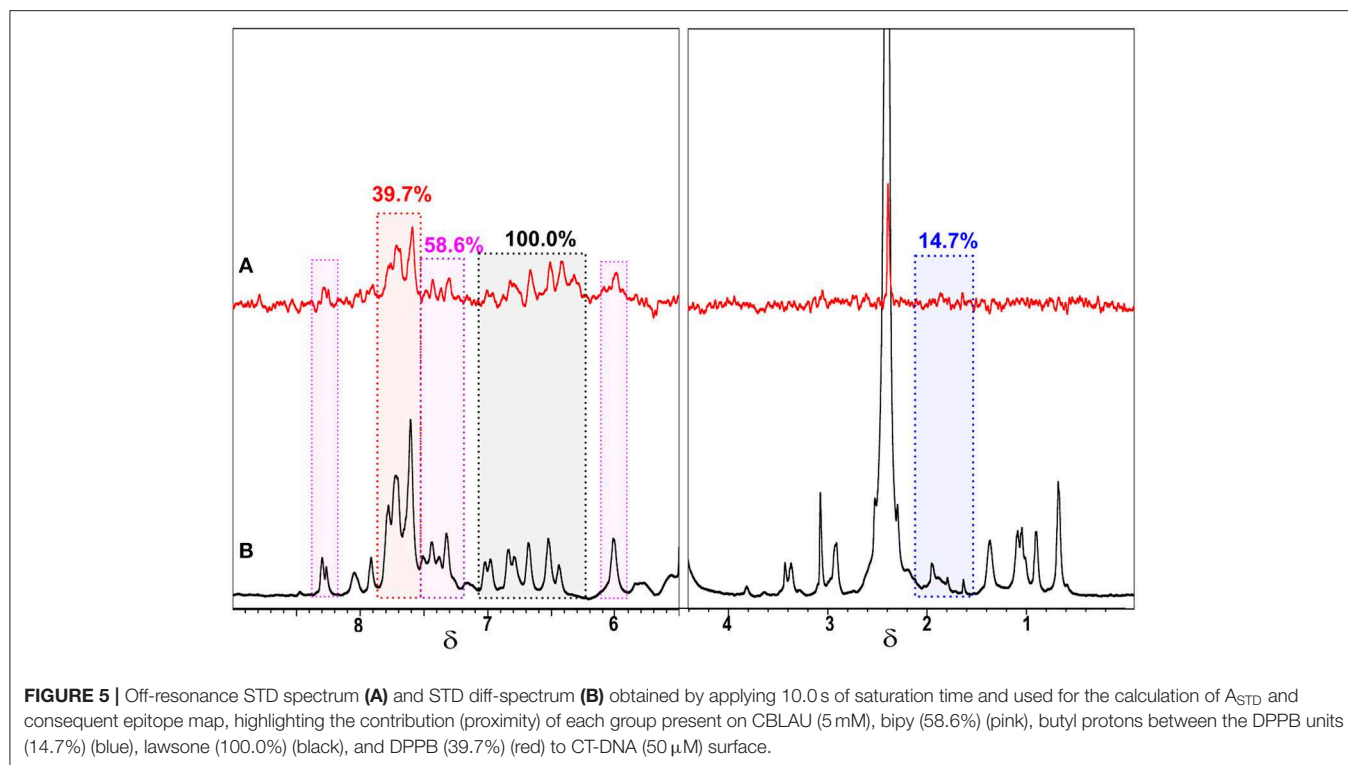
Despite these positive results of these relaxometry based binding-target experiments in demonstrating the interaction of CBLAU with CT-DNA, the T_1 relaxation times could change due to other effects, such as the viscosity variation. On the other hand, the T_1 variation is different for each group complexed to ruthenium, as mentioned. In this scenario, the interaction between CBLAU and CT-DNA was investigated by STD-NMR experiments (Figure 5), which is more robust, and depends exclusively on the spatial contact of the molecules involved in the interaction. This experiment allows to estimate not only the most accessible sites of binding contact present but supplies the intensity of these interactions. The epitope map, which describes the spatial proximities between the small molecule (CBLAU and lawsone) and the macromolecular target (CT-DNA), was built up from the acquisition of 14 STD-NMR experiments, ranging the saturation times from 0 to 10 s. Once the data was collected, the STD amplification factor (A_{STD}) was calculated using the $\text{STD}_{\text{off-resonance}}$ (Figure 5A) and STD_{diff} (Figure 5B) spectra, and performing the ratio of these spectra, in agreement to Equation (1). For the signal with higher A_{STD} value was attributed the percentage of 100% and for the other protons, the A_{STD} values were calculated with relation to this initial consideration. Besides, the signal intensity, as observed in these figures, does not only reflects the relative amount of saturation transferred from CT-DNA to CBLAU *via* cross-relaxation (spin-diffusion), but also reflects the relative proximity of a respective proton from CBLAU to the biological target surface on the final adduct (Mayer and Meyer, 1999, 2001; Angulo et al., 2010; Angulo and Nieto, 2011; Viegas et al., 2011; Monaco et al., 2018). In addition, it is important to stress that, the signal intensities in STD-NMR spectrum strongly depends on the equilibrium established between the species involved in the interaction, with similarities to the enzymatic inhibition equilibrium. Therefore, as in agreement to literature, two factors are important in these terms, one is the concentration of the small molecule and the second is the saturation transfer from the macromolecule to the small molecule (Viegas et al., 2011; Tanoli et al., 2015, 2018; Monaco et al., 2018). In this context, it is expected that longer saturation times improve the saturation transfer in the limit governed by the timescale of the contact between the

protons from CBLAU closer to CT-DNA surface. Thus, as the CBLAU concentrations increase, the CT-DNA surface reaches some saturation and, as response, the STD signal intensities should increase (Tanoli et al., 2015, 2018).

Regarding the dependence of the equilibrium with the timescale of the intermolecular contact between CBLAU and CT-DNA several STD experiments were collected by varying the saturation time. Therefore, analyzing the $\text{STD}_{\text{off-resonance}}$ and STD_{diff} spectra a built-up curve was obtained ranging the saturation time from 0 to 10.0 s for each CBLAU group, as shown in Figure 6A, where the exponential growth and the intensity of the curve plateau reflects the proximity of each group to the CT-DNA surface. This analysis allows to reach a map of the proximities between the Ru-complex and the CT-DNA surface, and this is known as epitope map. The results show that the lawsone group is the closest one (100.0%) in comparison to Bipy (58.6%), DPPB (39.7%), and butyl groups (between DPPB units), 14.7%. The epitope map shows that the interaction involves peripheral CBLAU protons, as expected, and an important finding is that the metallic complex structure is preserved, as previously observed by ^1H -NMR data. But an initial question should be answered regarding the recognized biological activity of lawsone: does the complexation with a metallic center improve its activity? This is an important concerning to justify the Ru-complex preparation. At this point, several STD experiments were conducted for individual lawsone, following the same approach.

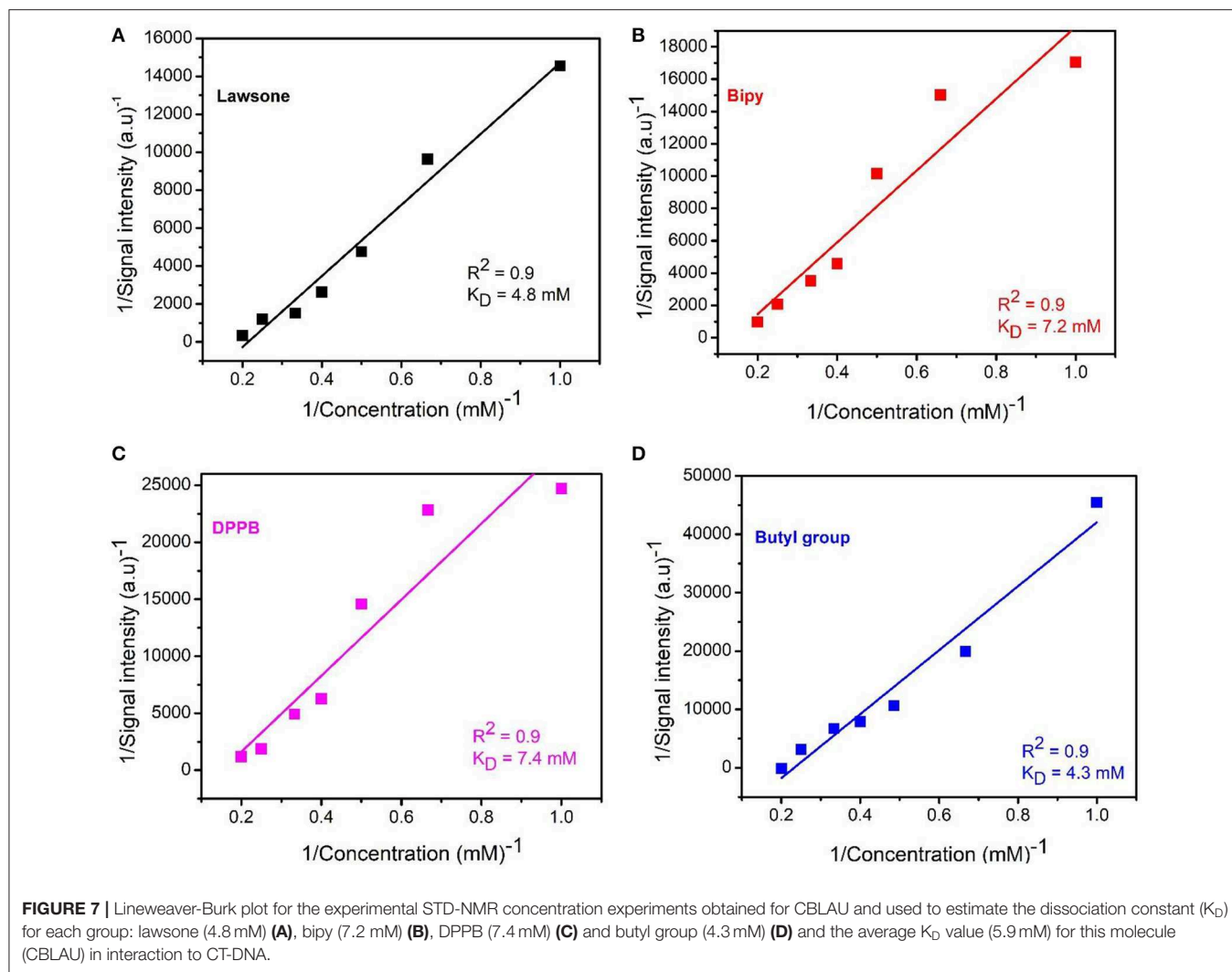
For the lawsone, STD experiments showed that the all aromatic protons are close to CT-DNA surface, as expected (Figure 6B). The proton 1 (green) refers to a lower (63.9%) A_{STD} value in comparison to the other protons, which A_{STD} values are quite similar: proton 2 (black) (100%), proton 3 (blue) (96.4%), proton 4 (pink) (94.3%), and proton 5 (red) (99.4%), respectively. Therefore, protons numbered from 2 to 5 are closer to CT-DNA and π - π stacking forces seem to govern the contact. Besides, these results reinforce that the presence of ligands containing aromatic groups on the design of anti-cancer candidates favors the contact with the DNA surface.

Interestingly, it is observed on Figure 6B that the A_{STD} values for the 2 to 5 protons of the non-Ru complexed lawsone exponentially increased until 10 s of saturation time, but differently to note for the CBLAU protons, the A_{STD} does not reach a stationary plateau, supposed at elevated saturation times conditions. These results indicate that besides these protons are closer to DNA, they are not completely saturated, in despite of the elevated saturation time, which is an additional indicative that the interaction of the non-Ru complexed lawsone with CT-DNA is weaker, in comparison to the Ru-complexed one. In addition, it is also observed for the proton 1 (green) on lawsone, that the A_{STD} values is more randomized in comparison to that one reached for another protons. These observations do not prevent the determination of A_{STD} , but demonstrate that the resonances close to solvent signal (4.7 ppm) are more influenced by the solvent suppression scheme used, where the excitation profile associated to the pulse sequence used also reduce the solvent nearby signals.



Nevertheless, a second question remains unanswered: how strong is the interaction between CBLAU and CT-DNA? To explore the quantitative aspects of the equilibrium established with interaction, the dissociation constants (K_D) were estimated for both cases: individual lawsone and Ru-complexed lawsone as in CBLAU. The estimation of K_D was performed by using several STD experiments, now varying the CBLAU concentration, in order to obtain a built-up curve, fitted by using a Lineweaver-Burk approach, as presented

in the experimental section. Notably, the Ru-complexed lawsone exhibits an average dissociation constant of 5.9 mM (Figure 7), which is much smaller than the average K_D obtained for non-Ru complexed lawsone:CT-DNA supramolecular adduct (34.0 mM) (Figure S1). To conclude it is quite clear that when complexed, the lawsone exhibits a stronger interaction with CT-DNA. Therefore, these results put light on the previously reported biological results (Oliveira et al., 2017a; Grandis et al., 2019), demonstrating that the CBLAU



complex interacts toward CT-DNA stronger than for non-Ru complexed lawsone.

CONCLUSIONS

The interaction between a novel anti-cancer candidate and the biological target DNA was understood at atomic level by NMR-binding approaches. The relaxometric results demonstrated to be an efficient probe to monitor the formation of CBLAU/CT-DNA adduct in solution and the T1 variation is bigger for lawsone and bipyridine groups. Besides, it was also demonstrated that this binding target interaction have a weak nature ($K_D = 5.9$ mM), experimentally proving the pivotal role assumed by the spatial contact, such as hydrogen bonding, hydrophobic contacts, hydrophilic-hydrophobic interactions and π - π stacking on the final adduct arrangement. The studies involving only the non-complexed lawsone suggests that the binding mode toward DNA occur in a similar way, but the interaction intensity is notably lower ($K_D = 34.0$ mM) in comparison to the Ru-complexed one. These results also reinforce the search for new metallic complexes

with organic molecules with recognized biological activity. The complexation with a metal can improves the interaction of these molecules with macromolecular biological targets. All these results put light on the reasons about the relevant biological features associated to this candidate against tumor cell lines DU-145 (prostate cancer cells), MCF-7 (breast cancer cells), A549 (lung cancer cells) as well as its potential to induce the tumor cells apoptosis. Therefore, we expect that these findings help the researchers working on bioinorganic to design new metallodrugs with improved activity and selectivity.

DATA AVAILABILITY STATEMENT

The datasets for this study are available on request to the corresponding author.

AUTHOR CONTRIBUTIONS

FK, AF, and TV designed the experiments. FK and TV generated and analyzed the experimental data. AC, KO, and

AB designed and synthesized the complex CBLAU and provided the non-complexed lawsonone. The manuscript was written by FK and TV. TV has supervised and finalized the final version of the manuscript.

FUNDING

The authors are gratefully acknowledged to the financial support from FAPESP (2018/19342-2, 2018/16040-5, and 2018/09145-5),

REFERENCES

- Ali, K. A., Abd-Elzaher, M. M., and Mahmoud, K. (2013). Synthesis and anticancer properties of Silver(I) complexes containing 2,6-Bis(substituted)pyridine derivatives. *Int. J. Med. Chem.* 2013, 256836–256842. doi: 10.1155/2013/256836
- Angulo, J., Enriquez-Navas, P. M., and Nieto, P. M. (2010). Ligand–receptor binding affinities from saturation transfer difference (STD) NMR spectroscopy: the binding isotherm of STD initial growth rates. *Chem. Eur. J.* 16, 7803–7812. doi: 10.1002/chem.200903528
- Angulo, J., and Nieto, P. M. (2011). STD-NMR: application to transient interactions between biomolecules—a quantitative approach. *Eur. Biophys. J.* 40, 1357–1369. doi: 10.1007/s00249-011-0749-5
- Chen, Z. F., Wu, Y. X., Zhu, Z. Z., and Zhang, Y. M. (2019). DNA cleavage, DNA/HAS binding study, and antiproliferative activity of activity of a phenolate-bridged binuclear copper (II) complex. *Biometals* 32, 227–240. doi: 10.1007/s10534-019-00172-w
- Dabiri, Y., Abu el Maaty, M. A., Chan, H. Y., Wolker, J., Ott, I., Wolf, S., et al. (2019). P53-dependent anti-proliferative and pro-apoptotic effects of a gold (I) N-heterocyclic (NHC) complex in colorectal cancer cells. *Front. Oncol.* 9:438. doi: 10.3389/fonc.2019.00438
- Engelbrecht, Z., Meijboom, R., and Cronje, M. J. (2018). The ability of silver (I) thiocyanate 4-methoxyphenyl phosphine to induce apoptotic cell death in esophageal cancer is correlated to mitochondrial perturbations. *Biometals* 31, 189–202. doi: 10.1007/s10534-017-0051-9
- Gagini, T., Colina-Vegas, L., Villareal, W., Borba-Santos, L. P., Pereira, C. S., Batista, A. A., et al. (2018). Metal-azole fungistatic drug complexes as anti-Sporothrix spp. agents. *New J. Chem.* 42, 13641–13650. doi: 10.1039/C8NJ01544A
- Grandis, R. A., Santos, P. W. S., Oliveira, K. M., Machado, A. R. T., Aissa, A. F., Batista, A. A., et al. (2019). Novel lawsonone-containing ruthenium(II) complexes: synthesis, characterization and anticancer activity on 2D and 3D spheroid models of prostate cancer cells. *Biorg. Chem.* 85, 455–468. doi: 10.1016/j.bioorg.2019.02.010
- Hua, S. X., Chen, F. H., Wang, X. Y., Wang, Y. J., and Gou, S. H. (2019). Pt(IV) hybrids containing a TDO inhibitor serve as potential anticancer immunomodulators. *J. Inorg. Biochem.* 195, 130–140. doi: 10.1016/j.jinorgbio.2019.02.004
- Hussaini, S. Y., Haque, R. A., and Razali, M. R. (2019). Recent progress in silver (I)-, gold (I)/(III)- and palladium (II)-N-heterocyclic carbene complexes: a review towards biological perspectives. *J. Organomet. Chem.* 882, 906–911. doi: 10.1016/j.jorganchem.2019.01.003
- Keller, J. (2011). *Understanding NMR Spectroscopy*. Chichester: John Wiley & Sons Ltd.
- Khan, S., Malla, A. M., Zafar, A., and Naseem, I. (2017). Synthesis of novel coumarin nucleus-based DPA drug-like molecular entity: *in vitro* DNA/Cu(II) binding, DNA cleavage and pro-oxidant mechanism for anticancer action. *PLoS ONE* 12:e0181783. doi: 10.1371/journal.pone.0181783
- Kosmider, B., and Osiecka, R. (2004). Flavonoid compounds: a review of anticancer properties and interactions with cis-diamminedichloroplatinum(II). *Drug Dev. Res.* 63, 200–211. doi: 10.1002/ddr.10421
- Levitt, M. (2008). *Spin Dynamics: Basics of Nuclear Magnetic Resonance*. Chichester: John Wiley & Sons Ltd.
- Lu, Y. Y., Shen, T., Yanh, H., and Gu, W. G. (2016). Ruthenium complexes induce HepG2 human hepatocellular carcinoma cell apoptosis and inhibit cell migration through regulation of the Nrf2 pathway. *Int. J. Mol. Sci.* 17, 775–785. doi: 10.3390/ijms17050775
- Makovec, T. (2019). Cisplatin and beyond: molecular mechanisms of action and drug resistance development in cancer chemotherapy. *Radiol. Oncol.* 53, 148–158. doi: 10.2478/raon-2019-0018
- Mayer, M., and Meyer, M. (1999). A fast and sensitive method to characterize ligand binding by saturation transfer difference NMR spectra. *Angew. Chem.* 111, 1902–1906.
- Mayer, M., and Meyer, M. (2001). Group epitope mapping (GEM) by STD NMR to identify segments of a ligand in direct contact with a protein receptor. *J. Am. Chem. Soc.* 123, 6108–6117. doi: 10.1021/ja0100120
- Monaco, S., Tailford, L. E., Juge, N., and Angulo, J. (2018). Differential epitope mapping by STD NMR spectroscopy to reveal the nature of protein–ligand contacts. *Angew. Chem. Int. Ed.* 57, 15289–15293. doi: 10.1002/anie.201707682
- Neprevishita, R., Monaco, S., Munoz-Garcia, J. C., Khimyak, Y. Z., and Angulo, J. (2019). Spatially resolved STD-NMR applied to the study of solute transport in biphasic systems: application to protein–ligand interactions. *Nat. Prod. Commun.* 14, 1934578–19849789. doi: 10.1177/1934578X19849789
- Oliveira, K. M., Correa, R. S., Barbosa, M. I. F., Ellena, J. A., Cominetti, M. R., and Batista, A. A. (2017b). Ruthenium(II)/triphenylphosphine complexes: an effective way to improve the cytotoxicity of lapachol. *Polyhedron* 130, 108–114. doi: 10.1016/j.poly.2017.04.005
- Oliveira, K. M., Luna-Dulcey, L., Correa, R. S., Deflon, V. M., Cominetti, M. R., and Batista, A. A. (2017a). Selective Ru(II)/lawsonone complexes inhibiting tumor cell growth by apoptosis. *J. Inorg. Biochem.* 176, 66–76. doi: 10.1016/j.jinorgbio.2017.08.019
- Oliveira, M. S., Barbosa, M. I. F., Souza, T. B., Moreira, D. R. M., Martins, F. T., Villareal, W., et al. (2019). A novel platinum complex containing a piplartine derivative exhibits enhanced cytotoxicity, causes oxidative stress and triggers apoptotic cell death by ERK/p38 pathway in human acute promyelocytic leukemia HL-60 cells. *Redox Biol.* 20, 182–194. doi: 10.1016/j.redox.2018.10.006
- Porsch, B., Laga, R., Horsky, J., Konak, C., and Ulbrich, K. (2009). Molecular weight and polydispersity of calf-thymus DNA: static light-scattering and size-exclusion chromatography with dual detection. *Biomacromolecules* 10, 3148–3150. doi: 10.1021/bm900768j
- Roy, S., Sil, A., and Chakraborty, T. (2019). Potentiating apoptosis and modulation of p53, Bcl2, and Bax by a novel chrysin ruthenium complex for effective chemotherapeutic efficacy against breast cancer. *J. Cell. Physiol.* 234, 4888–4909. doi: 10.1002/jcp.27287
- Siegel, R. L., Miller, K. D., and Jemal, A. (2019). Cancer statistics. *CA Cancer J. Clin.* 69, 7–34. doi: 10.3322/caac.21551
- Tanoli, N. U., Tanoli, S. A. K., Ferreira, A. G., Gul, S., Ul-Haq, Z. (2015). Evaluation of binding competition and group epitopes of acetylcholinesterase inhibitors by STD NMR, Tr-NOESY, DOSY and molecular docking: an old approach but new findings. *MedChemComm.* 6, 1882–1890. doi: 10.1039/C5MD00231A
- Tanoli, N. U., Tanoli, S. A. K., Ferreira, A. G., Mehmood, M., Gul, S., Monteiro, J. L., et al. (2018). Characterization of the interaction between coumarin-derivatives and acetylcholinesterase: examination by NMR and dock simulations. *J. Mol. Model.* 24:207. doi: 10.1007/s00894-018-3751-3
- Viegas, A., Manso, J., Nobrega, F. L., and Cabrita, E. J. (2011). Saturation-transfer difference (STD) NMR: a simple and fast method for ligand screening and characterization of protein binding. *J. Chem. Educ.* 88, 990–994. doi: 10.1021/ed101169t

SUPPLEMENTARY MATERIAL

The Supplementary Material for this article can be found online at: <https://www.frontiersin.org/articles/10.3389/fchem.2019.00762/full#supplementary-material>

- Villareal, W., Colina-Vegas, L., Visbal, G., Corona, O., Correa, R. S., Ellena, J., et al. (2017). Copper(I)-Phosphine polypyridyl complexes: synthesis, characterization, DNA/HSA binding study, and antiproliferative activity. *Inorg. Chem.* 56, 3781–3793. doi: 10.1021/acs.inorgchem.6b02419
- Wang, F. Y., Tang, X. M., Wang, X., Huang, K. B., Feng, H. M., Chen, Z. F., et al. (2018). Mitochondria-targeted platinum(II) complexes induce apoptosis-dependent autophagic cell death mediated by ER-stress in A549 cancer cells. *Eur. J. Med. Chem.* 155, 639–650. doi: 10.1016/j.ejmech.2018.06.018
- Yeo, C. I., Ooi, K. K., and Tiekink, E. R. T. (2018). Gold-based medicine: a paradigm shift in anti-cancer therapy? *Molecules* 23:E1410. doi: 10.3390/molecules23061410
- Zhang, C. T., Li, J., Qian, C. G., Luo, X. P., Wang, K. K., Zhao, P. X., et al. (2018). A multifunctional ternary Cu(II)-carboxylate polymeric nanocomplex for cancer thermochemotherapy. *Int. J. Pharm.* 549, 1–12. doi: 10.1016/j.ijpharm.2018.06.048

Conflict of Interest: The authors declare that the research was conducted in the absence of any commercial or financial relationships that could be construed as a potential conflict of interest.

Copyright © 2019 Kock, Costa, de Oliveira, Batista, Ferreira and Venâncio. This is an open-access article distributed under the terms of the Creative Commons Attribution License (CC BY). The use, distribution or reproduction in other forums is permitted, provided the original author(s) and the copyright owner(s) are credited and that the original publication in this journal is cited, in accordance with accepted academic practice. No use, distribution or reproduction is permitted which does not comply with these terms.